

Study of $B^0(\bar{B}^0) \rightarrow \pi^0\pi^0$, $B^\pm \rightarrow \pi^\pm\pi^0$ and $B^\pm \rightarrow K^\pm\pi^0$ decays

The BABAR Collaboration

February 7, 2008

Abstract

We present updated measurements of the branching fractions for the modes $B^0 \rightarrow \pi^0\pi^0$, $B^\pm \rightarrow \pi^\pm\pi^0$, and $B^\pm \rightarrow K^\pm\pi^0$. We also measure the time-integrated asymmetry $C_{\pi^0\pi^0}$ and the charge asymmetries $\mathcal{A}_{\pi^\pm\pi^0}$ and $\mathcal{A}_{K^\pm\pi^0}$. Based on a sample of approximately 227 million $B\bar{B}$ pairs collected by the BABAR detector at the PEP-II asymmetric-energy B Factory at SLAC, we measure

$$\mathcal{B}(B^0 \rightarrow \pi^0\pi^0) = (1.17 \pm 0.32 \pm 0.10) \times 10^{-6}, \quad C_{\pi^0\pi^0} = -0.12 \pm 0.56 \pm 0.06,$$

where the first errors are statistical and the second are systematic. The $B^0 \rightarrow \pi^0\pi^0$ signal has a significance of 4.9σ including systematic uncertainties. We also measure

$$\begin{aligned} \mathcal{B}(B^\pm \rightarrow \pi^\pm\pi^0) &= (5.8 \pm 0.6 \pm 0.4) \times 10^{-6}, \quad \mathcal{A}_{\pi^\pm\pi^0} = -0.01 \pm 0.10 \pm 0.02, \\ \mathcal{B}(B^\pm \rightarrow K^\pm\pi^0) &= (12.0 \pm 0.7 \pm 0.6) \times 10^{-6}, \quad \mathcal{A}_{K^\pm\pi^0} = 0.06 \pm 0.06 \pm 0.01. \end{aligned}$$

Using related BABAR measurements and isospin relations we find an upper bound on the angle difference $|\delta| = |\alpha - \alpha_{\text{eff}}|$ of 35° at the 90% C.L.

Submitted to the 32nd International Conference on High-Energy Physics, ICHEP 04,
 16 August—22 August 2004, Beijing, China

Stanford Linear Accelerator Center, Stanford University, Stanford, CA 94309

Work supported in part by Department of Energy contract DE-AC03-76SF00515.

The BABAR Collaboration,

B. Aubert, R. Barate, D. Boutigny, F. Couderc, J.-M. Gaillard, A. Hicheur, Y. Karyotakis, J. P. Lees,
V. Tisserand, A. Zghiche

Laboratoire de Physique des Particules, F-74941 Annecy-le-Vieux, France

A. Palano, A. Pompili

Università di Bari, Dipartimento di Fisica and INFN, I-70126 Bari, Italy

J. C. Chen, N. D. Qi, G. Rong, P. Wang, Y. S. Zhu

Institute of High Energy Physics, Beijing 100039, China

G. Eigen, I. Ofte, B. Stugu

University of Bergen, Inst. of Physics, N-5007 Bergen, Norway

G. S. Abrams, A. W. Borgland, A. B. Breon, D. N. Brown, J. Button-Shafer, R. N. Cahn, E. Charles,
C. T. Day, M. S. Gill, A. V. Gritsan, Y. Groysman, R. G. Jacobsen, R. W. Kadel, J. Kadyk, L. T. Kerth,
Yu. G. Kolomensky, G. Kukartsev, G. Lynch, L. M. Mir, P. J. Oddone, T. J. Orimoto, M. Pripstein,
N. A. Roe, M. T. Ronan, V. G. Shelkov, W. A. Wenzel

Lawrence Berkeley National Laboratory and University of California, Berkeley, CA 94720, USA

M. Barrett, K. E. Ford, T. J. Harrison, A. J. Hart, C. M. Hawkes, S. E. Morgan, A. T. Watson

University of Birmingham, Birmingham, B15 2TT, United Kingdom

M. Fritsch, K. Goetzen, T. Held, H. Koch, B. Lewandowski, M. Pelizaeus, M. Steinke
Ruhr Universität Bochum, Institut für Experimentalphysik 1, D-44780 Bochum, Germany

J. T. Boyd, N. Chevalier, W. N. Cottingham, M. P. Kelly, T. E. Latham, F. F. Wilson

University of Bristol, Bristol BS8 1TL, United Kingdom

T. Cuhadar-Donszelmann, C. Hearty, N. S. Knecht, T. S. Mattison, J. A. McKenna, D. Thiessen

University of British Columbia, Vancouver, BC, Canada V6T 1Z1

A. Khan, P. Kyberd, L. Teodorescu

Brunel University, Uxbridge, Middlesex UB8 3PH, United Kingdom

A. E. Blinov, V. E. Blinov, V. P. Druzhinin, V. B. Golubev, V. N. Ivanchenko, E. A. Kravchenko,
A. P. Onuchin, S. I. Serednyakov, Yu. I. Skovpen, E. P. Solodov, A. N. Yushkov

Budker Institute of Nuclear Physics, Novosibirsk 630090, Russia

D. Best, M. Bruinsma, M. Chao, I. Eschrich, D. Kirkby, A. J. Lankford, M. Mandelkern, R. K. Mommsen,
W. Roethel, D. P. Stoker

University of California at Irvine, Irvine, CA 92697, USA

C. Buchanan, B. L. Hartfiel

University of California at Los Angeles, Los Angeles, CA 90024, USA

S. D. Foulkes, J. W. Gary, B. C. Shen, K. Wang

University of California at Riverside, Riverside, CA 92521, USA

D. del Re, H. K. Hadavand, E. J. Hill, D. B. MacFarlane, H. P. Paar, Sh. Rahatlou, V. Sharma
University of California at San Diego, La Jolla, CA 92093, USA

J. W. Berryhill, C. Campagnari, B. Dahmes, O. Long, A. Lu, M. A. Mazur, J. D. Richman, W. Verkerke
University of California at Santa Barbara, Santa Barbara, CA 93106, USA

T. W. Beck, A. M. Eisner, C. A. Heusch, J. Kroseberg, W. S. Lockman, G. Nesom, T. Schalk,
 B. A. Schumm, A. Seiden, P. Spradlin, D. C. Williams, M. G. Wilson
University of California at Santa Cruz, Institute for Particle Physics, Santa Cruz, CA 95064, USA

J. Albert, E. Chen, G. P. Dubois-Felsmann, A. Dvoretzskii, D. G. Hitlin, I. Narsky, T. Piatenko,
 F. C. Porter, A. Ryd, A. Samuel, S. Yang
California Institute of Technology, Pasadena, CA 91125, USA

S. Jayatilke, G. Mancinelli, B. T. Meadows, M. D. Sokoloff
University of Cincinnati, Cincinnati, OH 45221, USA

T. Abe, F. Blanc, P. Bloom, S. Chen, W. T. Ford, U. Nauenberg, A. Olivas, P. Rankin, J. G. Smith,
 J. Zhang, L. Zhang
University of Colorado, Boulder, CO 80309, USA

A. Chen, J. L. Harton, A. Soffer, W. H. Toki, R. J. Wilson, Q. Zeng
Colorado State University, Fort Collins, CO 80523, USA

D. Altenburg, T. Brandt, J. Brose, M. Dickopp, E. Feltresi, A. Hauke, H. M. Lacker, R. Müller-Pfefferkorn,
 R. Nogowski, S. Otto, A. Petzold, J. Schubert, K. R. Schubert, R. Schwierz, B. Spaan, J. E. Sundermann
Technische Universität Dresden, Institut für Kern- und Teilchenphysik, D-01062 Dresden, Germany

D. Bernard, G. R. Bonneaud, F. Brochard, P. Grenier, S. Schrenk, Ch. Thiebaux, G. Vasileiadis, M. Verderi
Ecole Polytechnique, LLR, F-91128 Palaiseau, France

D. J. Bard, P. J. Clark, D. Lavin, F. Muheim, S. Playfer, Y. Xie
University of Edinburgh, Edinburgh EH9 3JZ, United Kingdom

M. Andreotti, V. Azzolini, D. Bettoni, C. Bozzi, R. Calabrese, G. Cibinetto, E. Luppi, M. Negrini,
 L. Piemontese, A. Sarti
Università di Ferrara, Dipartimento di Fisica and INFN, I-44100 Ferrara, Italy

E. Treadwell
Florida A&M University, Tallahassee, FL 32307, USA

F. Anulli, R. Baldini-Ferrolì, A. Calcaterra, R. de Sangro, G. Finocchiaro, P. Patteri, I. M. Peruzzi,
 M. Piccolo, A. Zallo
Laboratori Nazionali di Frascati dell'INFN, I-00044 Frascati, Italy

A. Buzzo, R. Capra, R. Contri, G. Crosetti, M. Lo Vetere, M. Macri, M. R. Monge, S. Passaggio,
 C. Patrignani, E. Robutti, A. Santroni, S. Tosi
Università di Genova, Dipartimento di Fisica and INFN, I-16146 Genova, Italy

S. Bailey, G. Brandenburg, K. S. Chaisanguanthum, M. Morii, E. Won
Harvard University, Cambridge, MA 02138, USA

- R. S. Dubitzky, U. Langenegger
Universität Heidelberg, Physikalisches Institut, Philosophenweg 12, D-69120 Heidelberg, Germany
- W. Bhimji, D. A. Bowerman, P. D. Dauncey, U. Egede, J. R. Gaillard, G. W. Morton, J. A. Nash,
M. B. Nikolich, G. P. Taylor
Imperial College London, London, SW7 2AZ, United Kingdom
- M. J. Charles, G. J. Grenier, U. Mallik
University of Iowa, Iowa City, IA 52242, USA
- J. Cochran, H. B. Crawley, J. Lamsa, W. T. Meyer, S. Prell, E. I. Rosenberg, A. E. Rubin, J. Yi
Iowa State University, Ames, IA 50011-3160, USA
- M. Biasini, R. Covarelli, M. Pioppi
Università di Perugia, Dipartimento di Fisica and INFN, I-06100 Perugia, Italy
- M. Davier, X. Giroux, G. Grosdidier, A. Höcker, S. Laplace, F. Le Diberder, V. Lepeltier, A. M. Lutz,
T. C. Petersen, S. Plaszczynski, M. H. Schune, L. Tantot, G. Wormser
Laboratoire de l'Accélérateur Linéaire, F-91898 Orsay, France
- C. H. Cheng, D. J. Lange, M. C. Simani, D. M. Wright
Lawrence Livermore National Laboratory, Livermore, CA 94550, USA
- A. J. Bevan, C. A. Chavez, J. P. Coleman, I. J. Forster, J. R. Fry, E. Gabathuler, R. Gamet,
D. E. Hutchcroft, R. J. Parry, D. J. Payne, R. J. Sloane, C. Touramanis
University of Liverpool, Liverpool L69 7ZE, United Kingdom
- J. J. Back,¹ C. M. Cormack, P. F. Harrison,¹ F. Di Lodovico, G. B. Mohanty¹
Queen Mary, University of London, E1 4NS, United Kingdom
- C. L. Brown, G. Cowan, R. L. Flack, H. U. Flaecher, M. G. Green, P. S. Jackson, T. R. McMahon,
S. Ricciardi, F. Salvatore, M. A. Winter
*University of London, Royal Holloway and Bedford New College, Egham, Surrey TW20 0EX,
United Kingdom*
- D. Brown, C. L. Davis
University of Louisville, Louisville, KY 40292, USA
- J. Allison, N. R. Barlow, R. J. Barlow, P. A. Hart, M. C. Hodgkinson, G. D. Lafferty, A. J. Lyon,
J. C. Williams
University of Manchester, Manchester M13 9PL, United Kingdom
- A. Farbin, W. D. Hulsbergen, A. Jawahery, D. Kovalskyi, C. K. Lae, V. Lillard, D. A. Roberts
University of Maryland, College Park, MD 20742, USA
- G. Blaylock, C. Dallapiccola, K. T. Flood, S. S. Hertzbach, R. Kofler, V. B. Koptchev, T. B. Moore,
S. Saremi, H. Staengle, S. Willocq
University of Massachusetts, Amherst, MA 01003, USA

¹Now at Department of Physics, University of Warwick, Coventry, United Kingdom

R. Cowan, G. Sciolla, S. J. Sekula, F. Taylor, R. K. Yamamoto
Massachusetts Institute of Technology, Laboratory for Nuclear Science, Cambridge, MA 02139, USA

D. J. J. Mangeol, P. M. Patel, S. H. Robertson
McGill University, Montréal, QC, Canada H3A 2T8

A. Lazzaro, V. Lombardo, F. Palombo
Università di Milano, Dipartimento di Fisica and INFN, I-20133 Milano, Italy

J. M. Bauer, L. Cremaldi, V. Eschenburg, R. Godang, R. Kroeger, J. Reidy, D. A. Sanders, D. J. Summers,
H. W. Zhao
University of Mississippi, University, MS 38677, USA

S. Brunet, D. Côté, P. Taras
Université de Montréal, Laboratoire René J. A. Lévesque, Montréal, QC, Canada H3C 3J7

H. Nicholson
Mount Holyoke College, South Hadley, MA 01075, USA

N. Cavallo,² F. Fabozzi,² C. Gatto, L. Lista, D. Monorchio, P. Paolucci, D. Piccolo, C. Sciacca
Università di Napoli Federico II, Dipartimento di Scienze Fisiche and INFN, I-80126, Napoli, Italy

M. Baak, H. Bulten, G. Raven, H. L. Snoek, L. Wilden
*NIKHEF, National Institute for Nuclear Physics and High Energy Physics, NL-1009 DB Amsterdam,
The Netherlands*

C. P. Jessop, J. M. LoSecco
University of Notre Dame, Notre Dame, IN 46556, USA

T. Allmendinger, K. K. Gan, K. Honscheid, D. Hufnagel, H. Kagan, R. Kass, T. Pulliam, A. M. Rahimi,
R. Ter-Antonyan, Q. K. Wong
Ohio State University, Columbus, OH 43210, USA

J. Brau, R. Frey, O. Igonkina, C. T. Potter, N. B. Sinev, D. Strom, E. Torrence
University of Oregon, Eugene, OR 97403, USA

F. Colecchia, A. Dorigo, F. Galeazzi, M. Margoni, M. Morandin, M. Posocco, M. Rotondo, F. Simonetto,
R. Stroili, G. Tiozzo, C. Voci
Università di Padova, Dipartimento di Fisica and INFN, I-35131 Padova, Italy

M. Benayoun, H. Briand, J. Chauveau, P. David, Ch. de la Vaissière, L. Del Buono, O. Hamon,
M. J. J. John, Ph. Leruste, J. Malcles, J. Ocariz, M. Pivk, L. Roos, S. T'Jampens, G. Therin
*Universités Paris VI et VII, Laboratoire de Physique Nucléaire et de Hautes Energies, F-75252 Paris,
France*

P. F. Manfredi, V. Re
Università di Pavia, Dipartimento di Elettronica and INFN, I-27100 Pavia, Italy

²Also with Università della Basilicata, Potenza, Italy

P. K. Behera, L. Gladney, Q. H. Guo, J. Panetta
University of Pennsylvania, Philadelphia, PA 19104, USA

C. Angelini, G. Batignani, S. Bettarini, M. Bondioli, F. Bucci, G. Calderini, M. Carpinelli, F. Forti,
M. A. Giorgi, A. Lusiani, G. Marchiori, F. Martinez-Vidal,³ M. Morganti, N. Neri, E. Paoloni, M. Rama,
G. Rizzo, F. Sandrelli, J. Walsh
Università di Pisa, Dipartimento di Fisica, Scuola Normale Superiore and INFN, I-56127 Pisa, Italy

M. Haire, D. Judd, K. Paick, D. E. Wagoner
Prairie View A&M University, Prairie View, TX 77446, USA

N. Danielson, P. Elmer, Y. P. Lau, C. Lu, V. Miftakov, J. Olsen, A. J. S. Smith, A. V. Telnov
Princeton University, Princeton, NJ 08544, USA

F. Bellini, G. Cavoto,⁴ R. Faccini, F. Ferrarotto, F. Ferroni, M. Gaspero, L. Li Gioi, M. A. Mazzoni,
S. Morganti, M. Pierini, G. Piredda, F. Safai Tehrani, C. Voena
Università di Roma La Sapienza, Dipartimento di Fisica and INFN, I-00185 Roma, Italy

S. Christ, G. Wagner, R. Waldi
Universität Rostock, D-18051 Rostock, Germany

T. Adye, N. De Groot, B. Franek, N. I. Geddes, G. P. Gopal, E. O. Olaiya
Rutherford Appleton Laboratory, Chilton, Didcot, Oxon, OX11 0QX, United Kingdom

R. Aleksan, S. Emery, A. Gaidot, S. F. Ganzhur, P.-F. Giraud, G. Hamel de Monchenault, W. Kozanecki,
M. Legendre, G. W. London, B. Mayer, G. Schott, G. Vasseur, Ch. Yèche, M. Zito
DSM/Daphnia, CEA/Saclay, F-91191 Gif-sur-Yvette, France

M. V. Purohit, A. W. Weidemann, J. R. Wilson, F. X. Yumiceva
University of South Carolina, Columbia, SC 29208, USA

D. Aston, R. Bartoldus, N. Berger, A. M. Boyarski, O. L. Buchmueller, R. Claus, M. R. Convery,
M. Cristinziani, G. De Nardo, D. Dong, J. Dorfan, D. Dujmic, W. Dunwoodie, E. E. Elsen, S. Fan,
R. C. Field, T. Glanzman, S. J. Gowdy, T. Hadig, V. Halyo, C. Hast, T. Hryn'ova, W. R. Innes,
M. H. Kelsey, P. Kim, M. L. Kocian, D. W. G. S. Leith, J. Libby, S. Luitz, V. Luth, H. L. Lynch,
H. Marsiske, R. Messner, D. R. Muller, C. P. O'Grady, V. E. Ozcan, A. Perazzo, M. Perl, S. Petrak,
B. N. Ratcliff, A. Roodman, A. A. Salnikov, R. H. Schindler, J. Schwiening, G. Simi, A. Snyder, A. Soha,
J. Stelzer, D. Su, M. K. Sullivan, J. Va'vra, S. R. Wagner, M. Weaver, A. J. R. Weinstein,
W. J. Wisniewski, M. Wittgen, D. H. Wright, A. K. Yarritu, C. C. Young
Stanford Linear Accelerator Center, Stanford, CA 94309, USA

P. R. Burchat, A. J. Edwards, T. I. Meyer, B. A. Petersen, C. Roat
Stanford University, Stanford, CA 94305-4060, USA

S. Ahmed, M. S. Alam, J. A. Ernst, M. A. Saeed, M. Saleem, F. R. Wappler
State University of New York, Albany, NY 12222, USA

³Also with IFIC, Instituto de Física Corpuscular, CSIC-Universidad de Valencia, Valencia, Spain

⁴Also with Princeton University, Princeton, USA

W. Bugg, M. Krishnamurthy, S. M. Spanier
University of Tennessee, Knoxville, TN 37996, USA

R. Eckmann, H. Kim, J. L. Ritchie, A. Satpathy, R. F. Schwitters
University of Texas at Austin, Austin, TX 78712, USA

J. M. Izen, I. Kitayama, X. C. Lou, S. Ye
University of Texas at Dallas, Richardson, TX 75083, USA

F. Bianchi, M. Bona, F. Gallo, D. Gamba
Università di Torino, Dipartimento di Fisica Sperimentale and INFN, I-10125 Torino, Italy

L. Bosisio, C. Cartaro, F. Cossutti, G. Della Ricca, S. Dittongo, S. Grancagnolo, L. Lanceri, P. Poropat,⁵
L. Vitale, G. Vuagnin
Università di Trieste, Dipartimento di Fisica and INFN, I-34127 Trieste, Italy

R. S. Panvini
Vanderbilt University, Nashville, TN 37235, USA

Sw. Banerjee, C. M. Brown, D. Fortin, P. D. Jackson, R. Kowalewski, J. M. Roney, R. J. Sobie
University of Victoria, Victoria, BC, Canada V8W 3P6

H. R. Band, B. Cheng, S. Dasu, M. Datta, A. M. Eichenbaum, M. Graham, J. J. Hollar, J. R. Johnson,
P. E. Kutter, H. Li, R. Liu, A. Mihalyi, A. K. Mohapatra, Y. Pan, R. Prepost, P. Tan, J. H. von
Wimmersperg-Toeller, J. Wu, S. L. Wu, Z. Yu
University of Wisconsin, Madison, WI 53706, USA

M. G. Greene, H. Neal
Yale University, New Haven, CT 06511, USA

⁵Deceased

1 INTRODUCTION

The study of B meson decays into charmless hadronic final states is important for the understanding of CP violation in the B system. In the Standard Model, CP violation arises from a single phase in the Cabibbo-Kobayashi-Maskawa quark-mixing matrix $V_{\text{q}q'}$ [1]. Measurements of the time-dependent CP -violating asymmetry in the $B^0 \rightarrow \pi^+\pi^-$ decay mode by the *BABAR* and Belle collaborations [2, 3] provide information on the angle $\alpha \equiv \arg[-V_{\text{td}}V_{\text{tb}}^*/V_{\text{ud}}V_{\text{ub}}^*]$ of the Unitarity Triangle. However, in contrast to the theoretically clean determination of the angle β in B^0 decays to charmonium final states [4, 5], the extraction of α in $B^0 \rightarrow \pi^+\pi^-$ is complicated by the interference of tree and penguin amplitudes with different weak phases. The difference between the angles α and α_{eff} , where α_{eff} is derived from the measured time-dependent $B^0 \rightarrow \pi^+\pi^-$ CP asymmetry, may be evaluated using measurements of the isospin-related decays $B^0(\bar{B}^0) \rightarrow \pi^0\pi^0$ and $B^\pm \rightarrow \pi^\pm\pi^0$ [6]. The amplitudes A^{ij} for the $B \rightarrow \pi^i\pi^j$ decays satisfy the relation

$$A^{+0} = \frac{1}{\sqrt{2}}A^{+-} + A^{00}, \quad (1)$$

and a similar relation for the conjugate amplitudes \bar{A}^{+-} , \bar{A}^{00} and $\bar{A}^{+0} = A^{-0}$.

For $B^0 \rightarrow \pi^0\pi^0$, the CP -related quantity that can be accessed experimentally is the time-integrated asymmetry $C_{\pi^0\pi^0}$, defined as

$$C_{\pi^0\pi^0} = \frac{1 - |\lambda_{00}|^2}{1 + |\lambda_{00}|^2}, \quad (2)$$

where $|\lambda_{00}| = |\bar{A}_{00}/A_{00}|$ is the modulus of the ratio of $B^0 \rightarrow \pi^0\pi^0$ and $\bar{B}^0 \rightarrow \pi^0\pi^0$ decay amplitudes. $C_{\pi^0\pi^0}$ may deviate from zero if the tree and penguin amplitudes are of comparable size and have different weak and strong phases. For B^\pm modes, the CP -violating charge asymmetry is defined as

$$\mathcal{A}_{CP} = \frac{|\bar{A}|^2 - |A|^2}{|\bar{A}|^2 + |A|^2}, \quad (3)$$

where A (\bar{A}) is the B^+ (B^-) decay amplitude. In the Standard Model, the decay $B^\pm \rightarrow \pi^\pm\pi^0$ is governed by a pure tree amplitude; as a result no charge asymmetry is expected. Both the rate and asymmetry of the decay $B^\pm \rightarrow K^\pm\pi^0$ may be used to extract useful constraints on penguin contributions to the $B \rightarrow K\pi$ amplitudes.

In this paper, we report a measurement of the time-integrated CP asymmetry in the $B^0 \rightarrow \pi^0\pi^0$ decay, and an updated measurement of the $B^0 \rightarrow \pi^0\pi^0$ branching fraction [7]. We also update the $B^\pm \rightarrow \pi^\pm\pi^0$ and $B^\pm \rightarrow K^\pm\pi^0$ branching fractions and charge asymmetries [8]. This study is based on $(226.6 \pm 2.5) \times 10^6$ $\Upsilon(4S) \rightarrow B\bar{B}$ decays (on-resonance data), collected with the *BABAR* detector. We also use approximately 16 fb^{-1} of data recorded 40 MeV below the $B\bar{B}$ pair production threshold (off-resonance data).

2 THE *BABAR* DETECTOR AND PARTICLE SELECTION

BABAR is a solenoidal detector optimized for the asymmetric-energy beams at PEP-II and is described in detail in Ref. [9]. Charged particle (track) momenta are measured with a 5-layer double-sided silicon vertex tracker and a 40-layer drift chamber inside a 1.5-T superconducting

solenoidal magnet. Neutral cluster (photon) positions and energies are measured with an electromagnetic calorimeter (EMC) consisting of 6580 CsI(Tl) crystals. The photon energy resolution is $\sigma_E/E = \{2.3/E(\text{GeV})^{1/4} \oplus 1.9\} \%$, and the angular resolution from the interaction point is $\sigma_\theta = 3.9^\circ/\sqrt{E(\text{GeV})}$. The photon energy scale is determined using symmetric $\pi^0 \rightarrow \gamma\gamma$ decays. Charged hadrons are identified with a detector of internally reflected Cherenkov light (DIRC) and using ionization measurements in the tracking detectors. An instrumented magnetic-flux return detects neutral hadrons and identifies muons. High efficiency for recording $B\bar{B}$ events in which one B decays with low multiplicity is achieved with a two-level trigger with complementary tracking-based and calorimetry-based trigger decisions.

Candidate π^0 mesons are reconstructed as pairs of photons, spatially separated in the EMC, with an invariant mass m_{π^0} satisfying $110 < m_{\pi^0} < 160 \text{ MeV}/c^2$. The resolution is approximately $8 \text{ MeV}/c^2$ for high momentum π^0 's. Photon candidates are required to be consistent with the expected lateral shower shape, not be matched to a track, and have a minimum energy of 30 MeV . To reduce the background from false π^0 candidates, the angle θ_γ between the photon momentum vector in the π^0 rest frame and the π^0 momentum vector in the laboratory frame is required to satisfy $|\cos \theta_\gamma| < 0.95$.

Candidate tracks are required to be within the tracking fiducial volume, originate from the interaction point, consist of at least 12 DCH hits, and be associated with at least 6 Cherenkov photons in the DIRC.

3 ANALYSIS METHOD

B meson candidates are reconstructed by combining a π^0 with a pion or kaon (h^\pm) or by combining two π^0 mesons. Two kinematic variables, used to isolate the $B^0 \rightarrow \pi^0\pi^0$ and $B^\pm \rightarrow h^\pm\pi^0$ signal events, take advantage of the kinematic constraints of B mesons produced at the $\Upsilon(4S)$. The first is the beam-energy-substituted mass $m_{\text{ES}} = \sqrt{(s/2 + \mathbf{p}_i \cdot \mathbf{p}_B)^2/E_i^2 - \mathbf{p}_B^2}$, where \sqrt{s} is the total e^+e^- center-of-mass (CM) energy, (E_i, \mathbf{p}_i) is the four-momentum of the initial e^+e^- system and \mathbf{p}_B is the B candidate momentum, both measured in the laboratory frame. The second variable is $\Delta E = E_B - \sqrt{s}/2$, where E_B is the B candidate energy in the CM frame. The ΔE resolution for signal is approximately 80 MeV for $B^0 \rightarrow \pi^0\pi^0$, and 40 MeV for $B^\pm \rightarrow h^\pm\pi^0$.

The primary source of background is $e^+e^- \rightarrow q\bar{q}$ ($q = u, d, s, c$) events where a π^0 or h^\pm from each quark randomly combines to mimic a B decay. The jet-like $q\bar{q}$ background is suppressed by requiring that the angle θ_s between the sphericity axes of the B candidate and that of the remaining tracks and photons in the event, in the CM frame, satisfies $|\cos \theta_s| < 0.7 (0.8)$ for $B^0 \rightarrow \pi^0\pi^0$ ($B^\pm \rightarrow h^\pm\pi^0$). The other sources of background are B to vector-pseudoscalar decays: $B^\pm \rightarrow \rho^\pm\pi^0$ for the $B^0 \rightarrow \pi^0\pi^0$ mode; $B^0 \rightarrow \rho^\pm\pi^\mp$, $B^\pm \rightarrow \rho^0\pi^\pm$, and $B^\pm \rightarrow \rho^\pm\pi^0$ for the $B^\pm \rightarrow \pi^\pm\pi^0$ mode; and $B^0 \rightarrow \rho^\pm K^\mp$, $B^\pm \rightarrow K^{*\pm}\pi^0$, and $B^0 \rightarrow K^{*0}\pi^0$ for the $B^\pm \rightarrow K^\pm\pi^0$ mode. In these decays the vector meson is polarized, so one of the pions is often produced almost at rest in the B rest frame, and the remaining decay products match the kinematics of a $B^0 \rightarrow \pi^0\pi^0$ or $B^\pm \rightarrow h^\pm\pi^0$ decay.

For the $B^0 \rightarrow \pi^0\pi^0$ analysis we restrict the $m_{\text{ES}} - \Delta E$ plane to the region with $m_{\text{ES}} > 5.2 \text{ GeV}/c^2$ and $|\Delta E| < 0.4 \text{ GeV}$. For the on-resonance sample we define the signal region as the band in the plane with $|\Delta E| < 0.2 \text{ GeV}$ and the sideband region as the rest of the plane with the exception of a region at negative ΔE also populated with $B^\pm \rightarrow \rho^\pm\pi^0$ events. The entire plane for the off-resonance data and the sideband region for the on-resonance data are populated with $q\bar{q}$ background events, which are kept in the fit in order to constrain the corresponding background

parameters. $B^\pm \rightarrow h^\pm \pi^0$ candidates are selected in the region with $m_{\text{ES}} > 5.22 \text{ GeV}/c^2$ and $-0.11 < \Delta E < 0.15 \text{ GeV}$.

For $B^0 \rightarrow \pi^0 \pi^0$ candidates, the other tracks and clusters in the event are used to determine whether the other B meson (B_{tag}) decayed as a B^0 or \bar{B}^0 (flavor tag). We use a multivariate technique [10] to determine the flavor of the B_{tag} meson. Separate neural networks are trained to identify primary leptons, kaons, soft pions from D^* decays, and high-momentum charged particles from B decays. Each event is assigned to one of several mutually exclusive tagging categories based on the estimated mistag probability and on the source of tagging information.

The number of signal B candidates is determined in an extended unbinned maximum likelihood fit. The probability $\mathcal{P}_i(\vec{x}_j; \vec{\alpha}_i)$ for a signal or background hypothesis is the product of probability density functions (PDFs) for the variables \vec{x}_j given the set of parameters $\vec{\alpha}_i$. The likelihood function is given by a product over the N events and the M signal and background hypotheses:

$$\mathcal{L} = \exp \left(- \sum_{i=1}^M n_i \right) \prod_{j=1}^N \left[\sum_{i=1}^M N_i \mathcal{P}_i(\vec{x}_j; \vec{\alpha}_i) \right]. \quad (4)$$

For $B^0 \rightarrow \pi^0 \pi^0$ the coefficients N_i are given by $N_i = \frac{1}{2}(1 - s_j \mathcal{A}_i)n_i$, where s_j refers to the sign of the flavor tag of the other B in the event j and is zero for untagged events. n_i and \mathcal{A}_i are the number of events and raw asymmetry for $B^0 \rightarrow \pi^0 \pi^0$ signal, $B^\pm \rightarrow \rho^\pm \pi^0$ background, and continuum background components. The averages of the $B^\pm \rightarrow \rho^\pm \pi^0$ branching fraction and asymmetry [11, 12] are used to fix the number of $B^+ \rightarrow \rho^+ \pi^0$ and $B^- \rightarrow \rho^- \pi^0$ events to 32.1 ± 5.6 . The asymmetry $\mathcal{A}_{\pi^0 \pi^0}$ is related to the time-integrated CP asymmetry $C_{\pi^0 \pi^0}$ by the relation

$$\mathcal{A}_{\pi^0 \pi^0} = (1 - 2\chi)(1 - 2\omega)C_{\pi^0 \pi^0}, \quad (5)$$

where $\chi = 0.186 \pm 0.004$ [13] is the time-integrated mixing probability, and ω is the mis-tagging probability. Asymmetries in mistag rates and efficiencies are taken into account.

For $B^\pm \rightarrow h^\pm \pi^0$ the probability coefficients are $N_i = \frac{1}{2}(1 - q_j \mathcal{A}_i)n_i$, where q_j is the charge of the track h in the event j , and the fit parameters n_i and \mathcal{A}_i are the number of events and asymmetry for $B^\pm \rightarrow \pi^\pm \pi^0$ and $B^\pm \rightarrow K^\pm \pi^0$ signal, continuum, and B background components. The numbers of B background events are fixed to the expected number of events using the current world averages for the $\rho\pi$ [11, 12, 14, 15, 16] and ρK [16] decays, which are 18 ± 4 and 3 ± 1 events, respectively. We estimate a contribution of 1 ± 1 $B \rightarrow K^* \pi^0$ events to the background based on the upper limit on the branching fraction [17]. The uncertainties on these numbers are dominated by the uncertainty on selection efficiencies, because of the sensitivity to the tight requirement in ΔE .

The variables \vec{x}_j used for $B^0 \rightarrow \pi^0 \pi^0$ are m_{ES} , ΔE , and a Fisher discriminant \mathcal{F} . The Fisher discriminant is an optimized linear combination of $\sum_i p_i$ and $\sum_i p_i \cos^2 \theta_i$, where p_i is the momentum and θ_i is the angle with respect to the thrust axis of the B candidate, both in the CM frame, for all tracks and neutral clusters not used to reconstruct the B meson. For both the $B^0 \rightarrow \pi^0 \pi^0$ signal and the $B^\pm \rightarrow \rho^\pm \pi^0$ background the m_{ES} and ΔE variables are correlated and therefore a two-dimensional PDF from a smoothed, simulated distribution is used. For the continuum background, the m_{ES} distribution is modeled as a threshold function [18], whose shape parameter ξ is free in the fit, and the ΔE distribution as a quadratic function whose parameters are free in the fit. The PDF for the \mathcal{F} variable is modeled as a parametric step function (PSF)[7] for all event components. A PSF is a binned distribution whose parameters are the heights of each bin. The PSF is normalized to one, so that the number of free parameters is equal to the number of bins minus one. The \mathcal{F} PSF

has ten bins chosen so that each bin contains 10% of the signal sample. For the $B^0 \rightarrow \pi^0\pi^0$ signal and the $B^\pm \rightarrow \rho^\pm\pi^0$ background the \mathcal{F} PSF parameters are correlated with the flavor tagging, and the PSF parameters are different for each tagging category. Simulation is used to determine the PSF distributions for both $B^0 \rightarrow \pi^0\pi^0$ and $B^\pm \rightarrow \rho^\pm\pi^0$. A sample of $B \rightarrow D^{(*)}n\pi$ ($n = 1, 2, 3$) events is used to verify that the simulation reproduces the \mathcal{F} distribution. For $q\bar{q}$ background, the \mathcal{F} PSF parameters are free parameters in the fit.

The variables \vec{x}_j used for $B^\pm \rightarrow h^\pm\pi^0$ are m_{ES} , ΔE , the Cherenkov angle θ_c of the h^\pm track, and the Fisher discriminant \mathcal{F} . The PDF parameters for m_{ES} , ΔE , θ_c , and \mathcal{F} for the background are determined using the data, while the PDFs for signal are found from a combination of simulated events and data. The m_{ES} and ΔE distributions for $q\bar{q}$ events are treated as in the $B^0 \rightarrow \pi^0\pi^0$ case, with parameters allowed to vary freely in the fit. For the signal, the m_{ES} and ΔE distributions are both modeled as a Gaussian distribution with a low-side power law tail whose parameters are determined from simulation. The mean of the signal m_{ES} and ΔE distributions are determined from the fit to the $B^\pm \rightarrow h^\pm\pi^0$ sample and their values used to tune the π^0 energy scale in the $B^0 \rightarrow \pi^0\pi^0$ analysis. The mean of ΔE for the $B^\pm \rightarrow K^\pm\pi^0$ mode is a function of the kaon laboratory momentum, since a pion mass hypothesis is used. The distribution of \mathcal{F} is modeled as a bifurcated Gaussian for the signal, whose parameters are obtained from simulation, and as a double Gaussian for the continuum background, whose parameters are determined in the likelihood fit. The difference of the measured and expected values of θ_c for the pion or kaon hypothesis, divided by the uncertainty on θ_c , is modeled as a double Gaussian function. A control sample of kaon and pion tracks, from the decay $D^{*+} \rightarrow D^0\pi^+$, $D^0 \rightarrow K^-\pi^+$, is used to parameterize σ_{θ_c} as a function of the charged track momentum.

4 RESULTS AND SYSTEMATIC UNCERTAINTIES

The result of the maximum likelihood fit for $B^0 \rightarrow \pi^0\pi^0$ is $n(B^0 \rightarrow \pi^0\pi^0) = 61 \pm 17$ (see Table 1). The statistical significance of the event yield is evaluated from the square root of the change in $-2\ln\mathcal{L}$ between the nominal fit and a separate fit in which the signal yield is fixed to zero, and is found to be 5.2σ (statistical errors only). The time-integrated asymmetry is $C_{\pi^0\pi^0} = -0.12 \pm 0.56$. Distributions of likelihood fit variables for $B^0 \rightarrow \pi^0\pi^0$ are shown in Fig. 1. The data shown are for events that have passed a probability ratio cut optimized to enhance the signal to background fraction. A validation is made by performing a simpler event-counting analysis, based on the number of $B^0 \rightarrow \pi^0\pi^0$ candidates satisfying tighter requirements. The result of the event-counting analysis is $n(B^0 \rightarrow \pi^0\pi^0) = 43 \pm 26$ and agrees well with the result from the maximum likelihood fit. This result is statistically consistent with our previously reported measurement [7]. With changes in the analysis technique to measure the CP asymmetry, we now find 44 ± 13 events in the first 123 million $B\bar{B}$ events, compared to 46 ± 13 events found in Ref. [7]. The additional 104 million $B\bar{B}$ events dataset has a signal of 17 ± 11 events. The signal rates in these two subsets agree at the 1.3σ level. This result also includes an improved understanding of the π^0 detection efficiency. Using a sample of π^0 mesons from $\tau^\pm \rightarrow \pi^\pm\pi^0\nu_\tau$ decays we establish a π^0 efficiency correction of $\varepsilon_\pi^0 = 0.99 \pm 0.03$ to our GEANT simulation, compared to a correction of 0.88 ± 0.08 in Ref. [7].

For $B^\pm \rightarrow h^\pm\pi^0$ the results are $n(B^\pm \rightarrow \pi^\pm\pi^0) = 379 \pm 41$ and $n(B^\pm \rightarrow K^\pm\pi^0) = 682 \pm 39$. The charge asymmetries are $\mathcal{A}_{\pi^\pm\pi^0} = -0.01 \pm 0.10$ and $\mathcal{A}_{K^\pm\pi^0} = 0.06 \pm 0.06$. Results are summarized in Table 1. Distributions of likelihood fit variables for $B^\pm \rightarrow h^\pm\pi^0$ are shown in Fig. 2.

Systematic uncertainties on the event yields and CP asymmetries are evaluated on data control samples, or by varying the fixed parameters and refitting the data. Tables 2 and 3 summarize

the dominant contributions to the systematic uncertainties for the $B^0 \rightarrow \pi^0\pi^0$ and $B^\pm \rightarrow h^\pm\pi^0$ branching fractions and asymmetries. For $B^0 \rightarrow \pi^0\pi^0$, the dominant systematics arise from the uncertainty on the ΔE resolution and the efficiency of the π^0 reconstruction. We reevaluate the significance of the $B^0 \rightarrow \pi^0\pi^0$ signal from zero, including all systematic effects in the direction which reduces the signal, and find a significance of 4.9σ .

For both $B^\pm \rightarrow \pi^\pm\pi^0$ and $B^\pm \rightarrow K^\pm\pi^0$, the dominant systematic uncertainties arise from the \mathcal{F} PDF parameters for signal, selection efficiencies, and the ΔE resolution. Additional systematic uncertainties arise from the EMC energy scale, selection efficiencies, and particle identification. The systematic uncertainty on the charge asymmetries is dominated by the upper limit of the charge bias in the detector (1.0%) [19], since most selection and PDF systematics cancel in the asymmetry.

We use the isospin relations, Eq. 1, to extract information on the angle difference $\delta = \alpha - \alpha_{\text{eff}}$ [6], in conjunction with the *BABAR* measurements of $C_{\pi^+\pi^-} = (-0.09 \pm 0.15 \pm 0.04)$ [2], the branching fraction $\mathcal{B}(B^0 \rightarrow \pi^+\pi^-) = (4.7 \pm 0.6 \pm 0.2) \times 10^{-6}$ [20], the $B^0 \rightarrow \pi^0\pi^0$ and $B^\pm \rightarrow \pi^\pm\pi^0$ decay rates and the $C_{\pi^0\pi^0}$ asymmetry described in this paper. We scan over all values of $|\delta|$ and calculate a χ^2 for the five amplitudes (A^{+-} , \bar{A}^{+-} , A^{00} , \bar{A}^{00} and A^{+0}), given these five measurements and the two constraints (Eq. 1 and its conjugate) for each value of $|\delta|$. The χ^2 is converted into a confidence level, as shown in Fig. 3, from which we derive an upper bound on $|\delta|$ of 35° at the 90% C.L.

5 CONCLUSION

We observe $61 \pm 17 \pm 5$ $B^0 \rightarrow \pi^0\pi^0$ events with a significance of 4.9σ including systematic uncertainties. This corresponds to a branching fraction $\mathcal{B}(B^0 \rightarrow \pi^0\pi^0) = (1.17 \pm 0.32 \pm 0.10) \times 10^{-6}$, where the first error is statistical and the second is systematic. We measure the time-integrated asymmetry $C_{\pi^0\pi^0} = -0.12 \pm 0.56 \pm 0.06$. We report branching fractions $\mathcal{B}(B^\pm \rightarrow \pi^\pm\pi^0) = (5.8 \pm 0.6 \pm 0.4) \times 10^{-6}$ and $\mathcal{B}(B^\pm \rightarrow K^\pm\pi^0) = (12.0 \pm 0.7 \pm 0.6) \times 10^{-6}$. The charge asymmetries are $\mathcal{A}_{\pi^\pm\pi^0} = -0.01 \pm 0.10 \pm 0.02$ and $\mathcal{A}_{K^\pm\pi^0} = 0.06 \pm 0.06 \pm 0.01$; we find no evidence for CP violation. These results are consistent with our previous results for these decays [7, 8]. We find an upper bound on the angle difference $\delta = \alpha - \alpha_{\text{eff}}$ of $|\delta| < 35^\circ$ at the 90% C.L.

6 ACKNOWLEDGMENTS

We are grateful for the extraordinary contributions of our PEP-II colleagues in achieving the excellent luminosity and machine conditions that have made this work possible. The success of this project also relies critically on the expertise and dedication of the computing organizations that support *BABAR*. The collaborating institutions wish to thank SLAC for its support and the kind hospitality extended to them. This work is supported by the US Department of Energy and National Science Foundation, the Natural Sciences and Engineering Research Council (Canada), Institute of High Energy Physics (China), the Commissariat à l’Energie Atomique and Institut National de Physique Nucléaire et de Physique des Particules (France), the Bundesministerium für Bildung und Forschung and Deutsche Forschungsgemeinschaft (Germany), the Istituto Nazionale di Fisica Nucleare (Italy), the Foundation for Fundamental Research on Matter (The Netherlands), the Research Council of Norway, the Ministry of Science and Technology of the Russian Federation, and the Particle Physics and Astronomy Research Council (United Kingdom). Individuals have received support from CONACyT (Mexico), the A. P. Sloan Foundation, the Research Corporation, and the Alexander von Humboldt Foundation.

Table 1: The results for the modes $B^0 \rightarrow \pi^0 \pi^0$ and $B^\pm \rightarrow h^\pm \pi^0$ are summarized. For each mode, the sample size N , number of signal events N_S , total detection efficiency ε , branching fraction \mathcal{B} , asymmetry \mathcal{A} or $C_{\pi^0 \pi^0}$, and 90% confidence interval for the asymmetry are shown. For $C_{\pi^0 \pi^0}$ the confidence interval is normalized to the physical region $[-1, 1]$. Errors are statistical and systematic respectively, with the exception of ε whose error is purely systematic.

Mode	N	N_S	ε (%)	$\mathcal{B}(10^{-6})$	Asymmetry	(90% C.L.)
$B^0 \rightarrow \pi^0 \pi^0$	8153	61 ± 17	23.5 ± 1.4	$1.17 \pm 0.32 \pm 0.10$	$-0.12 \pm 0.56 \pm 0.06$	$[-0.88, 0.64]$
$B^\pm \rightarrow \pi^\pm \pi^0$	29950	379 ± 41	28.7 ± 1.1	$5.8 \pm 0.6 \pm 0.4$	$-0.01 \pm 0.10 \pm 0.02$	$[-0.19, 0.21]$
$B^\pm \rightarrow K^\pm \pi^0$	13165	682 ± 39	25.0 ± 1.0	$12.0 \pm 0.7 \pm 0.6$	$0.06 \pm 0.06 \pm 0.01$	$[-0.06, 0.18]$

Table 2: Systematic uncertainties in the determination of the $B^0 \rightarrow \pi^0 \pi^0$ branching fraction (left), and the $C_{\pi^0 \pi^0}$ asymmetry (right). In order of decreasing importance the branching fraction is affected by the uncertainties in the efficiency (3% for each π^0), in the difference between simulation and data of the ΔE resolution, in the branching fraction $B^\pm \rightarrow \rho^\pm \pi^0$, and in the number of produced $B\bar{B}$ pairs. The systematic uncertainty on $C_{\pi^0 \pi^0}$ is dominated by the uncertainty on the B background asymmetry.

Source	$\Delta\mathcal{B}(\pi^0 \pi^0)$		Source	$\Delta(C_{\pi^0 \pi^0})$
π^0 efficiency	+6%	-6%	B background asymmetry	± 0.05
ΔE resolution	+7.2%	-1.0%	tagging efficiency	± 0.03
$\mathcal{B}(B \rightarrow \rho\pi)$	+3.4%	-3.1%	simulation	± 0.02
mean of ΔE and m_{ES}	+1.5%	-1.6%	$\mathcal{B}(B \rightarrow \rho\pi)$	± 0.01
luminosity	+1.1%	-1.1%		

Table 3: Dominant systematic uncertainties for $B^\pm \rightarrow \pi^\pm \pi^0$ and $B^\pm \rightarrow K^\pm \pi^0$, listed in order of decreasing importance as percent changes in the branching fractions \mathcal{B} (left), and absolute changes in the asymmetries $\mathcal{A}_{\pi^\pm \pi^0}$, $\mathcal{A}_{K^\pm \pi^0}$ (right).

Source	$\Delta\mathcal{B}(\pi^\pm \pi^0)$	$\Delta\mathcal{B}(K^\pm \pi^0)$	Source	$\Delta(\mathcal{A}_{\pi^\pm \pi^0})$	$\Delta(\mathcal{A}_{K^\pm \pi^0})$
\mathcal{F} , ΔE simulation	$\pm 4.2\%$	$\pm 3.3\%$	detector bias	± 0.010	± 0.010
π^0 efficiency	$\pm 3.1\%$	$\pm 3.1\%$	\mathcal{F} , ΔE simulation	± 0.011	± 0.007
B background	$\pm 2.2\%$	$\pm 0.2\%$	B background	± 0.008	± 0.001
luminosity	$\pm 1.1\%$	$\pm 1.1\%$	h^\pm identification	± 0.004	± 0.003
h^\pm identification	$\pm 0.5\%$	$\pm 0.6\%$			

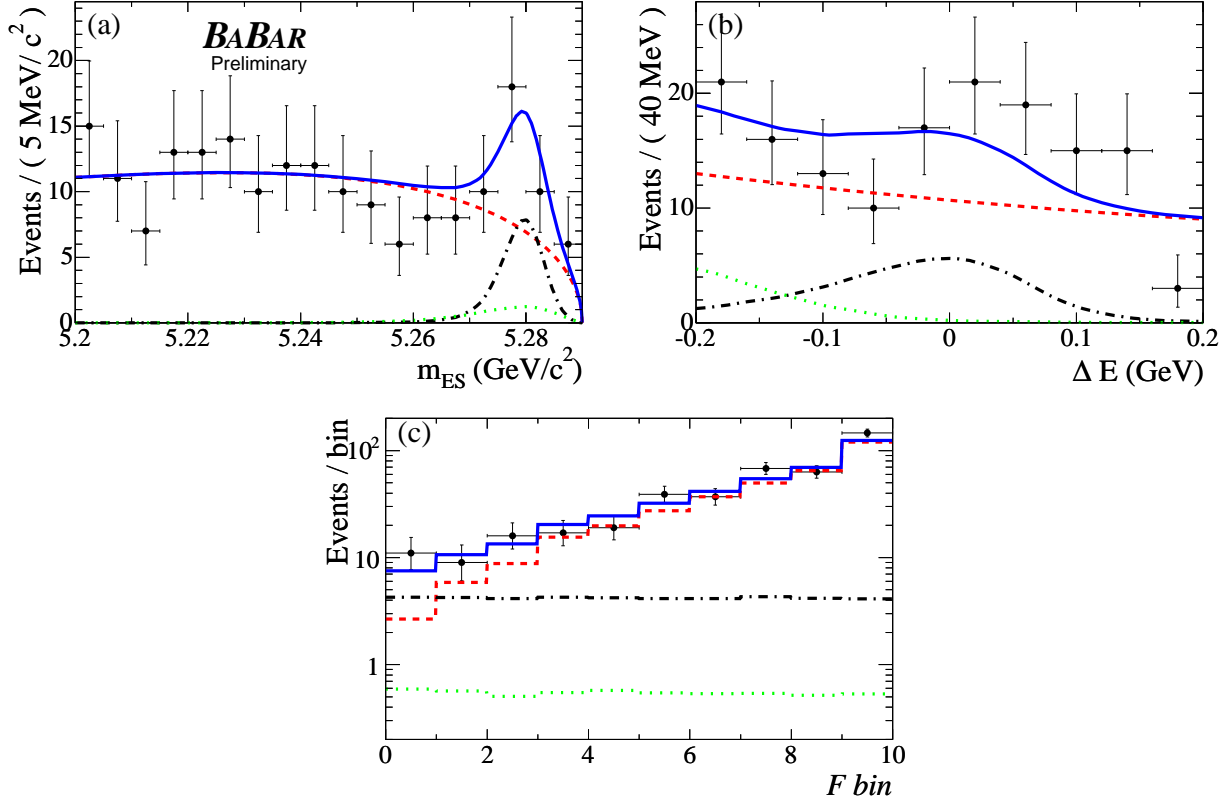


Figure 1: The distributions of (a) m_{ES} , (b) ΔE , and (c) Fisher discriminant \mathcal{F} for $B^0 \rightarrow \pi^0 \pi^0$ candidates in the signal data sample that satisfy an optimized requirement on the signal probability, based on all variables except the one being plotted. The projections contain 25%, 45% and 68% of the signal, 14%, 31% and 17% of the $\rho\pi^0$ background, and 2.2%, 1.3% and 4.4% of the continuum background, for m_{ES} , ΔE , and \mathcal{F} respectively. The PDF projections are shown as a dashed line for $q\bar{q}$ background, a dotted line for $B^\pm \rightarrow \rho^\pm \pi^0$, and a dashed-dotted line for $B^0 \rightarrow \pi^0 \pi^0$ signal. The solid line shows the sum of all PDF projections. The PDF projections are scaled by the expected fraction of events passing the probability-ratio requirement.

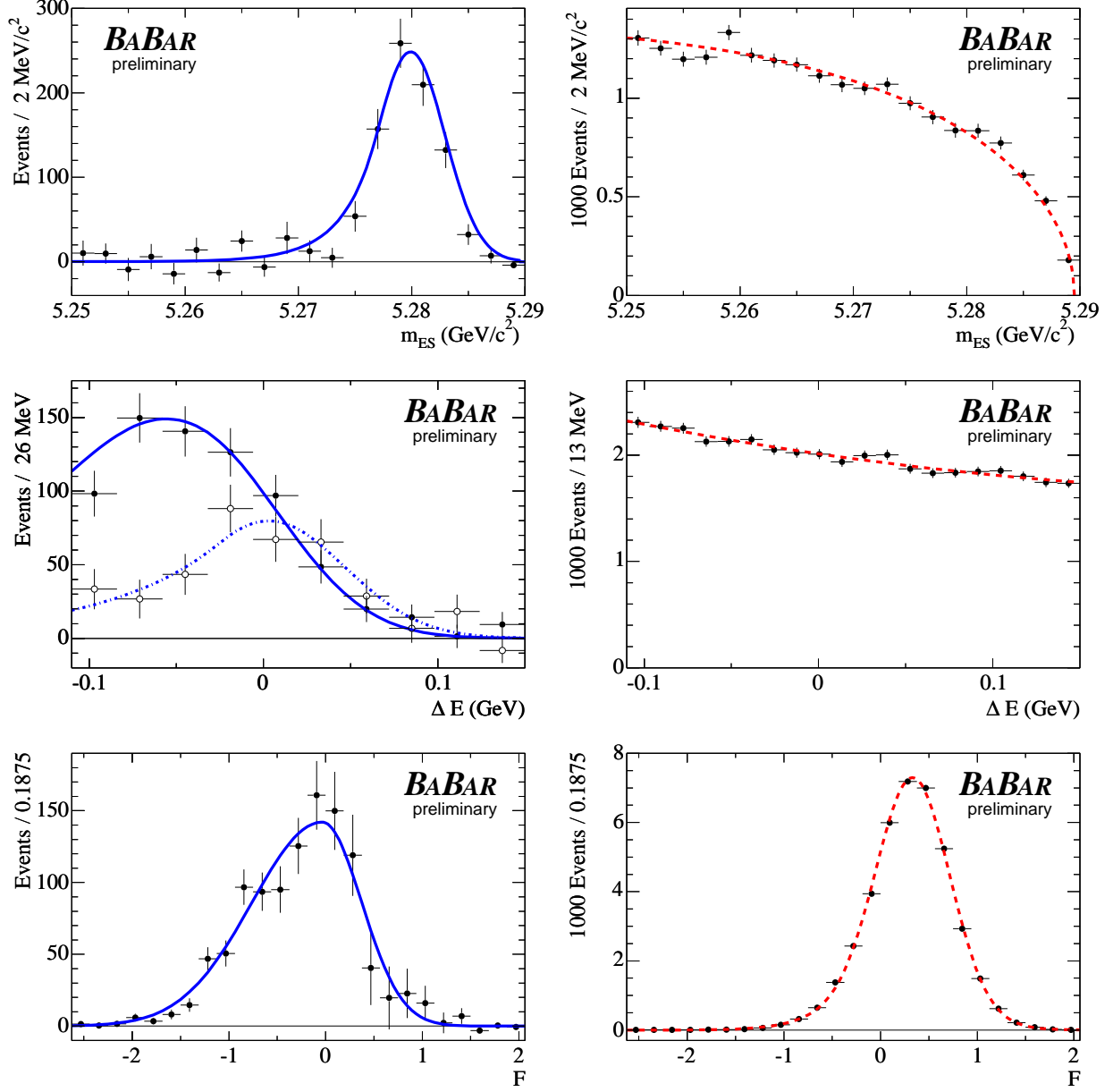


Figure 2: The distributions and PDF projections of m_{ES} (top), ΔE (middle) and \mathcal{F} discriminant (bottom), for $B^\pm \rightarrow \pi^\pm \pi^0$ and $B^\pm \rightarrow K^\pm \pi^0$ candidates in the data sample. Figures on the left are for background-subtracted signal events, and background distributions are on the right. For m_{ES} and \mathcal{F} discriminant, the $B^\pm \rightarrow \pi^\pm \pi^0$ and $B^\pm \rightarrow K^\pm \pi^0$ distributions are combined, while for signal ΔE the $B^\pm \rightarrow \pi^\pm \pi^0$ (open circles and dotted dashed curve) and $B^\pm \rightarrow K^\pm \pi^0$ (solid circles and solid curve) distributions are shown separately. The background is subtracted using the method described in reference [21]. The method uses all variables except the one being plotted.

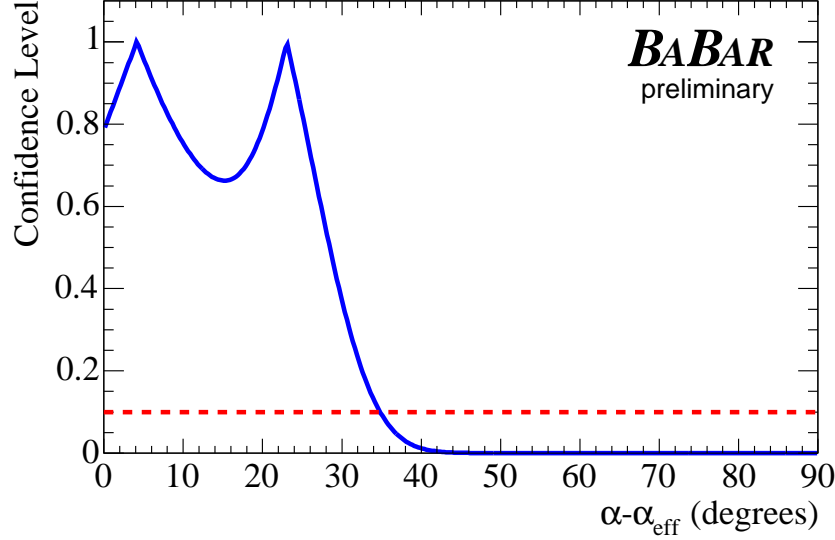


Figure 3: Constraints on the angle $\delta = \alpha - \alpha_{\text{eff}}$, expressed as a Confidence Level as a function of $|\delta|$. The constraint is evaluated using the isospin relations (Eq. 1) and the *BABAR* measurements of the $B \rightarrow \pi\pi$ branching fractions and the CP violation parameters $C_{\pi^0\pi^0}$ and $C_{\pi^+\pi^-}$. We find an upper bound on $|\delta|$ of 35° at the 90% C.L.

References

- [1] N. Cabibbo, Phys. Rev. Lett. **10**, 531 (1963); M. Kobayashi and T. Maskawa, Prog. Theor. Phys. **49**, 652 (1973).
- [2] *BABAR* Collaboration, B. Aubert *et al.*, CONF-04/047, Contribution to ICHEP 2004.
- [3] Belle Collaboration, K. Abe *et al.*, Phys. Rev. Lett. **93**, 021601 (2004).
- [4] *BABAR* Collaboration, B. Aubert *et al.*, Phys. Rev. Lett. **89**, 201802 (2002).
- [5] Belle Collaboration, K. Abe *et al.*, Phys. Rev. D **66**, 071102 (2002).
- [6] M. Gronau and D. London, Phys. Rev. Lett. **65**, 3381 (1990).
- [7] *BABAR* Collaboration, B. Aubert *et al.*, Phys. Rev. Lett. **91**, 241801 (2003).
- [8] *BABAR* Collaboration, B. Aubert *et al.*, Phys. Rev. Lett. **91**, 021801 (2003).
- [9] *BABAR* Collaboration, B. Aubert *et al.*, Nucl. Instrum. Methods **A479**, 1 (2002).
- [10] *BABAR* Collaboration, B. Aubert *et al.*, Phys. Rev. D **66**, 032003 (2002).
- [11] *BABAR* Collaboration, B. Aubert *et al.*, hep-ex/0311049 to be published in Phys. Rev. Lett.
- [12] Belle Collaboration, J. Zhang, *et al.*, hep-ex/0406006 to be published in Phys. Rev. Lett.

- [13] Particle Data Group, S. Eidelman *et al.*, Phys. Lett. B **592**, 1 (2004).
- [14] Belle Collaboration, A. Gordon *et al.*, Phys. Lett. B **542**, 183 (2002).
- [15] CLEO Collaboration, C.P. Jessop, *et al.*, Phys. Rev. Lett. **85**, 2881 (2000).
- [16] BABAR Collaboration, B. Aubert *et al.*, Phys. Rev. Lett. **93**, 051802 (2004).
- [17] BABAR Collaboration, B. Aubert *et al.*, CONF-04/042, Contribution to ICHEP 2004.
- [18] The threshold function used for the m_{ES} PDF is $\frac{m_{\text{ES}}}{m_0} \sqrt{1 - (\frac{m_{\text{ES}}}{m_0})^2} \exp \left\{ -\xi \left[1 - (\frac{m_{\text{ES}}}{m_0})^2 \right] \right\}$, where m_0 is the m_{ES} endpoint, and ξ the shape parameter. See ARGUS Collaboration, H. Albrecht *et al.*, Z. Phys. C **48**, 543 (1990).
- [19] BABAR Collaboration, B. Aubert *et al.*, Phys. Rev. D **65**, 051101 (2002).
- [20] BABAR Collaboration, B. Aubert *et al.*, Phys. Rev. Lett. **89**, 281802 (2002).
- [21] F. Le Diberder and M. Pivk, LAL 04-07, physics/0402083.